ASTEROID IMPACT CONNECTIONS OF CRUSTAL EVOLUTION*

ANDREW Y GLIKSON† AND JOHN VICKERS

Research School of Earth Science & School of Archaeology and Anthropology, Australian National University, Canberra, Australian Capital Territory, 0200, Australia.

***In memory of Shen Su Sun* (1943 – 2005)**

† Andrew.glikson@anu.edu.au   61 2 6296 3853

Advances in isotopic age determinations increasingly point to an episodic nature of the evolution of lithosphere and crust. The purpose of this paper is to review well documented field and geochemical evidence which indicates that, at least some of these episodes were associated with large asteroid impacts. Observed overlaps between early Precambrian impacts (~3.47 Ga, ~2.63 Ga, ~2.56 Ga, ~2.48 Ga, ~2.023 Ga [Vredefort] and 1.85 Ga [Sudbury]) and isotopic age frequency peaks, defined within age errors, while not constituting proof of cause-effect relationships, invite tests of field evidence relevant to this question. Evidence for major dynamic and thermal effects of large impact clusters on the early Precambrian crust is provided by ejecta fallout units associated with (1) unconformities; (2) tsunami boulder debris; (3) compositional contrasts between supracrustal sequences which underlie and overlie the ejecta units; (4) onset of episodes of iron-rich sedimentation, and (5) near-contemporaneous intrusion of granitoid magmas. An impact cluster ~3.26–3.24 Ga-old documented in the Barberton greenstone belt, South Africa, is associated with unconformities and granite activity correlated with unconformities and olistostromes in the Pilbara Craton, Western Australia. In both cratons a 300 million years-long period of greenstone-granite evolution is terminated abruptly by unconformities overlain by impact ejecta, turbidite and banded iron formations. The 3.26 and 3.24 Ga terminations involve major faulting, uplift, erosion, and onset of high-energy sedimentation which includes detrital components from contemporaneous granites. An onset of ferruginous sedimentation, including banded iron formations, in the wake of the ~3.47, ~3.26, ~3.24, ~2.63 and ~2.56 Ga impacts suggests weathering and soluble transport of ferrous oxide under low-oxidation atmosphere and hydrosphere conditions, possibly reflecting extensive mafic volcanic activity triggered by the impacts. Extensive dyke formation during 2.48–2.42 Ga (Matachewan, Scourie, Karelian, Widgiemooltha, Bangalore, Antarctica dykes) may be related to deep crust/mantle fractures triggered by the ~2.48 Dales Gorge mega-impact. Tentative observations are consistent with, but do not demonstrate, possible overlaps between Phanerozoic impacts and the onset of faulting and plate tectonics episodes

KEYWORDS: asteroid, impact, microkrystite, Archaean, early Proterozoic, crustal evolution

INTRODUCTION

Scientists studying extraterrestrial Impact events have long suspected that large asteroid impacts may have had a profound, hitherto unrecognized, effect on the history of the Earth crust (Dietz, 1964; Green, 1972, 1981; Grieve, 1980; Jones, 1987; Oberbeck et al., 1992; Boslough et al., 1994; Alt et al., 1998; Glikson, 1993, 1994, 1995, 2007A, 2008). Several authors pointed out circumstantial evidence for temporal relations between large asteroid impacts and major Phanerozoic faulting and onset of plate tectonic events, including stages in the break up of Gondwana (Alt et al., 1988; Oberbeck et al., 1992). These include correlations between large impact clusters, hot spots, continental basalts (Morgan, 1981; Richards et al., 1989; Courtillot et al., 1999), continental rifting and opening of oceanic gaps (Table 1).

Due to a dominant Earth-centric focus to date only limited account has been taken in most models of crustal evolution of the effects of large asteroid impacts (cf. Windley, 1977; Condie, 1995, Myers, 1995; Smithies et al., 2005; Van Kranendonk, 2007). Attempts to correlate Phanerozoic magmatic, rifting and plate tectonic events with large asteroid impacts (Hughs and McGetchin, 1977; Jones, 1987; Alt et al., 1988; Oberbeck et al., 1992; Marvin, 1990) based on unproven age overlaps, remain subject for tests by field work and precise age correlations.

Possible candidates for such tests include (Table 1):

A. Late Triassic asteroid bombardment (Manicouagan – ~214 Ma D: 100 km; Rochechouart ~213 Ma D: 23 km), succeeded by rifting of the Atlantic ocean at ~200 - 180 Ma.

B. Late Jurassic asteroid bombardment (Morokweng 145±0.8 Ma D: 70 km; Gosses Bluff 142.5±0.8 D: 24 km; Ma; Mjolnir 143±2.6 Ma D: 40 km) succeeded by stages of Gondwana break up.

C. End-Cretaceous impacts (Chicxulub 64.98±0.05 Ma D: 170 km; Boltysh 65.17±0.64 Ma D: 25 km); opening of the Indian-Arabian gulf.

In this paper I refer to the well-documented 3.26 – 3.24 Ga asteroid impact cluster in the Barberton greenstone belt, Kaapvaal Craton, South Africa (Lowe and Byerly, 1986; Lowe et al., 1989, 2003; Kyte et al., 1992; Byerly and Lowe, 1994; Shukolyukov et al., 2000; Glikson, 2007B), and contemporaneous events in the Pilbara Craton (Glikson and Vickers, 2005; Glikson, 2008), as a reference test case for potential relationships between large impact events and tectonic and magmatic events potentially triggered by these events.

PRECAMBRIAN ASTEROID IMPACTS

The Late Heavy Bombardment (LHB) of the Moon about 3.85-3.95 Gyr-ago (Ryder, 1990, 1991, 1997), evidenced by the large Mare basins (Imbrium, Tranquilitatis, Serenitatis, Crisium, Orientalis), are likely to have involved the Earth, coupled with the Moon during the first hundred million years of accretion from the solar nebula. On Earth the LHB must have terminated prior to the deposition of the Isua supracrustal sequence (~3.80 Ga; Nutman et al., 2007) and Akilia tonalite (~3.83 Ga; Mojzsis and Harrison, 2002) in South West Greenland, which to date disclose little evidence of large subsequent impacts.

However, the end of the LHB far from signifies the end of major extraterrestrial impact effects on Earth, with major impact events documented by impact ejecta units and by impact craters at ~3.46, 3.26, 3.24, 2.63, 2.56, 2.48, 2.023 and 1.85 Ga (Table 2). The discovery of millimeter-scale spherules in Archaean sediments in South Africa and Western Australia (Figures 1 and 2), identical with microkrystite spherules as defined by Glass and Burns (1988) from the 65 Myr-old Cretaceous-Tertiary asteroid impact boundary (Lowe and Byerly, 1986; Lowe et al., 1989, 2003; Kyte et al., 1992; Byerly and Lowe, 1994; Shukloyukov et al., 2000), has allowed new insights into the impact history of Earth pre-2.4 Ga.

Simonson and colleagues (Simonson, 1992; Simonson and Hassler, 1997; Simonson and Glass, 2004; Simonson et al., 2000, 2006) identified several impact spherule units and associated tsunami deposits of three different ages (2.63, 2.56, 2.48 Ga) in the Hamersley Basin of Western Australia and the Transvaal Basin, South Africa. Whereas field identification of microkrystites is hampered by their millimeter-scale, the common occurrence of tsunami deposits above the spherule units provides a helpful criterion (Simonson and Hassler, 1997; Glikson, 2004).

Microkrystite spherules are produced by condensation of impact-ejected vapor released when large bolides collide with Earth. On impact, target materials are shattered, brecciated, and the core surrounding the exploding bolide is evaporated. Crust and mantle underlying exploding projectile rebound elastically to form a dome (Grieve and Dence, 1979; Grieve and Shoemaker, 1994; Grieve and Pesonen, 1996;

Grieve and Pilkington, 1996; Shoemaker and Shoemaker, 1996; French, 1998). The impact vapor is dispersed in the atmosphere, transported by winds, cools and condenses as a myriad melt droplets solidified as tiny glass spheres preserved in submarine sediments (Glass and Burns, 1988; Melosh and Vickery, 1991)

Microkrystite spherules are distinguished from volcanic melt droplets formed by volcanic fountaining by virtue of their inward-radiating quench crystallites and centrally offset vesicles, evidence of aerodynamic imbalance (Figures 5D, 7B, 8C). Microkrystites may contain nickel-rich spinels, rare micron-scale metallic nuggets of nickel and platinum group elements, and geochemical and isotopic signatures including platinum group element anomalies including high iridium levels, high Ir/Pd ratios, and $^{53}Cr/^{52}Cr$ isotope anomalies (Kyte et al., 1992; Byerly et al., 1994; Shukolyukov et al., 2000; Simonson and Glass, 2004; Glikson, 2005A,B). Iridium, with chondritic abundance more than 3 orders of magnitude higher than in the Earth's mantle, provides the telltale clue used by Alvarez et al. (1982) to prove the impact connection of the K-T boundary 65 Myr-ago.

To date eight major Precambrian impacts and impact clusters have been identified in South Africa, Western Australia, Canada and Greenland (Table 2), indicating events at 3.47, 3.26, 3.24, 2.63, 2.56 and 2.48, 2.023 and 1.85 Ga. The impact ejecta units are closely associated with tsunami deposits, which range from cross beds (Figure 7C) to fragmented material and large erratic boulders and debris flow (Figures 1C, 1D, 5B, 5C), to in-situ disrupted submarine beds (Figure 6). In the case of the 2.63 Gyr Carawine Dolomite, where spherule-bearing megabreccia 20 to 30 metre thick extends over more than 100 kilometers (Simonson and Hassler, 1997; Glikson, 2004), the tsunami wave affected pelagic (below-wave-base) carbonates, testifying to possibly over 200 meter-deep wave amplitudes affecting the sea bed.

Geochemical mass balance calculations based on iridium and on chromium isotopes and on spherule size distributions (Melosh and Vickery, 1991), suggest asteroids about 20-50 km in diameter (Byerly and Lowe, 1994; Kyte et al., 1992; Shukloyukov et al., 2000; Glikson, 2005A), raising the question of the potential structural and magmatic effects of impacts on this scale. Lowe and Byerly (1989) noted a juxtaposition between multiple 3.26 - 3.24 Gyr-old impact fallout units in the Barberton greenstone belt and the boundary between ultrabasic volcanics of the Mendon Formation (Onverwacht Group) (3298±3 Ma; Byerly et al., 1995) and an overlying sequence of turbidities, sandstones, siliceous volcanics, banded ironstones and conglomerates of the Fig Tree (3259±3 Ma) and Moodies Groups (Figures 2). Given the estimated Eros-scale dimension of the parental asteroids (Eros: 33x13 km), could this impact cluster have triggered crust-mantle upheavals leading to the fundamental break in the evolution of the Barberton greenstone belt?

A search for equivalent 3.26-3.24 Gyr microkrystite spherule units in the Pilbara Craton, a needle in a haystack exercise, has shown that the approximate stratigraphic where the ~3.24 Ga impact spherule units may be found is overlain by a large boulder deposit, or olistostrome, including blocks up to 250 metre across (Glikson and Vickers, 2005) (Figure 3B), suggesting strong faulting and collapse. To date no microkrystite spherules were disclosed at this stratigraphic level, possibly due to the quartz-rich composition of sediments overlying the unconformity, i.e. between the underlying volcanic Sulphur Springs Group (3251-3235 Ma) and unconformably overlying arenites of the Soanesville Group (Hickman, 2004; Van Kranendonk et al., 2007). In both the Pilbara and the Barberton terrains major intrusion of granite magmas occurs at ~3.24 Ga. Age overlaps between large impacts, unconformities, breccias and tsunami events are listed in Table 3.

New evidence for potential connections between asteroid impacts and crustal events emerged when a 2.63 Ga Jeerinah Impact Layer was identified above the Jeerinah Shale (Simonson et al., 2000), directly beneath the Marra Mamba Iron Formation (Figures 4, 5C). Further investigations indicate that, likewise, the 3.47, 3.26, 3.24 and 2.56 Gyr-old impact ejecta layers are located below iron-rich sediments (Glikson, 2006; Glikson and Vickers, 2006). Under the low oxygen levels of the early atmosphere weathering of iron in its soluble divalent form (FeO) would occur, resulting in leaching, transportation, saturation and colloidal precipitation of iron-rich cherts and banded ironstones. The ferro-magnesian composition of the impact ejecta testifies to impacts impinging on sima-dominated crust, necessarily triggering catastrophic mantle melting beneath the impact basins and consequent mafic volcanism. Could the large volumes of ferrous iron contained in Archaean banded iron formations been derived by weathering of such volcanic rocks and iron-rich hydrothermal fluids?

A conceptual model of the relationships between the 3.26 – 3.24 Ga impact cluster and contemporaneous geodynamic events, culminating in emergence of continental nuclei, is portrayed in Figure 11. From the Mg and Fe-rich composition of the Barberton spherules (Lowe et al., 2003; Glikson, 2005B) and the paucity, with some exceptions (Rasmussen and Koeberl, 2004), of shocked quartz-rich ejecta, the asteroids likely impacted on mostly mafic crust. For an asteroid 20 to 50 kilometer in diameter, impact basins several hundreds kilometer large and several tens of kilometer deep would be excavated, piercing the Earth's mantle, triggering mantle rebound, mantle diapirs and massive volcanic activity, with possible rearrangement of mantle convection systems.

In terms of an impact model, recurrent episodic accretion of volcanics and sediments lasting over a period longer than 300 million years and accompanied with protracted intrusion of tonalite-trondhjemite-granodiorite plutons (Glikson 1972), was abruptly terminated by a mega-impact cluster. During this >300 million years-long period, high geothermal gradients in the range of 15 - 25^{o}C/km resulted in buoyancy of the oceanic crust, retardation of subduction and arrest or partially arrest of plate tectonic processes (Green, 1972, 1981). Lateral accretion of arc-trench-like volcanic rocks in post-3.2 Ga greenstone belts (Sleep, 2008) resulted in a zonation of age provinces, as in the Superior Province (Goodwin, 1974; Folinsbee et al., 1968; Card, 1990), West Pilbara Craton (Van Kranendonk et al., 2007), and part of the Yilgarn Craton (Mary Gee and Swager, 2008).

SIGNIFICANCE OF ISOTOPIC AGE FREQUENCY PEAKS

The origin of isotopic age frequency peaks has been interpreted alternatively in terms of episodic thermal and magmatic events, intermittent plate tectonics events, or mantle dynamics and plume activity (Davies, 1995; Condie, 1995; Smithies et al., 2005). A compilation of 5509 U-Pb zircon ages by O'Reilly et al. (2008) defines at least 9 prominent age distribution peaks at ~3336, ~3212, ~2675, ~2560, ~2030, ~1625, ~1165, ~570 and ~290 Ma (Figure 9). This includes 1680 zircon U-Pb age determinations with high initial δ^{176}Hf values signifying derivation of magmas from juvenile mantle with peaks at ~3336, ~3212, ~2750, ~2560, ~1650, ~1198, ~290 Ma. Mantle-derived magmas are distinguished from reworked crustal magmas by their high δ^{176}Hf values (>0.2807), which reflect high ^{176}Lu/^{177}Hf of >0.02 (Pietranik et al. 2008). The statistical significance and the origin of these peaks remain to be determined.

Davies (1995) modeled global thermodynamic peak events in terms of episodic mantle overturn events related to temporal cooling, changes in phase transformation barriers, changes in the mantle layering structure, and subduction of plates. In this model 1.0 to 2.0 Ga phase changes are correlated with peak thermodynamic events, with preferred model peaks at ~3.85, ~3.4, ~2.7, ~1.85, ~1.18 and ~1.05 Ga (Davies 1995, figure 5 model [a]). The model peaks correspond in part to the following events (Figure 9):

1. The ~3.85 Ga peak correlates with the end of the Late Heavy Bombardment (Ryder, 1990, 1991, 1997);
2. The ~3.4 Ga and ~2.7 Ga peaks correlate with periods of maximum volcanic activity in Archaean greenstone belts (Nelson, 2008);
3. The ~1.85 Ga peak correlates with the Sudbury mega-impact event (D ~ 250 km) (Davis, 2008) (Table 2) and with thermodynamic events in Proterozoic mobile belts, for example the Capricorn orogeny, Western Australia (Nelson, 2008);
4. The ~1.6 Ga and 1.18 Ga peaks correlate with extensive thermodynamic events in Proterozoic mobile belts, for example in northwestern Queensland and central Australia (O'Reilly et al., 2008).

However, U-Pb zircon age peaks at ~3.34, ~3.21, ~2.03, ~0.57 and ~0.29 Ga (O'Reilly et al., 2008; Nelson, 2008) are not expressed on Davies' (1995) model (a). These ages correlate with the following crustal events:

1. The ~3.34 Ga peak correlates with extensive volcanic activity (Euro Basalt, Pilbara Craton; Hickman, 2004; Hickman and Van Kranendonk, 2004; Van Kranendonk et al., 2007)
2. The ~3.21 Ga peak postdates the Barberton asteroid cluster of 3.26-3.24 (Figure 10) within error.
3. The ~2.03 Ga peak overlaps within error with the Vredefort mega-impact (D: 298 km), Kaapvaal Craton, and the Glenburgh orogeny in Western Australia (Nelson, 2008).

It appears that, whereas no single factor can be invoked for the observed isotopic age peaks, several Precambrian isotopic age frequency peaks indicated by up-to-date compilations of igneous and detrital zircon U-Pb ages (O'Reilly et al., 2008; Nelson, 2008; Poujol et al., 2003) overlap with major asteroid impact events:

~3.47-3.44 Ga: This period includes peak magmatic events in the Kaapvaal Craton (Poujol, et al., 2003) and in the Pilbara Craton (Nelson, 2008). An impact cluster event occurs at 3470.1±2.3 Ma (Byerly et al., 2002) within the felsic volcanic Hooggenoeg Formation (~3.47 – 3.44 Ga; Poujol et al., 2003), correlated with an impact cluster at the base of the Apex Basalt (Warrawoona Group), dated at 3470.1±1.9 Ma (Byerly et al., 2002; Glikson et al., 2004)

~3.212 Ga: This peak (O'Reilly et al., 2008) and peaks in the range of ~3.22 - 3.26 Ga (Poujol et al., 2003) (Figure 10) correspond to the asteroid impact cluster at the base of the Fig Tree Group, Barberton greenstone belt, which include impacts at ~3.24 Ga and ~3.26 Ga (Lowe et al., 2003; Glikson, 2008).

~2.675 – 2.56 Ga: This peak period includes the tentatively dated 2629±5 Ma Jeerinah Impact Layer (JIL) (Simonson et al., 2000) and the 2565±9 Ma Spherule Marker Bed, Hamersley Basin (Simonson, 1972) (the age of the JIL is uncertain as it is based on an unconfirmed stratigraphic correlation: A.F. Trendall, pers. Com.). Both impact units are overlain by ferruginous shale and banded iron formations, possibly signifying iron derived from mafic volcanic and hydrothermal activity (Glikson and Vickers, 2006). Western Australian age frequency data define peaks at 2.6 – 2.75 Ga (Figure 9).

The age of the SMB impact unit overlaps the Sm–Nd 2586±16 Ma age of the Zimbabwe Great Dyke (Mukasa et al., 1998), but is marginally younger than U–Pb ages of the dyke (2587±8 Ma; Mukasa et al., 1998; 2578±0.9 Ma; Collerson et al., 2002), and Re–Os ages (2576±1 Ma; Schoenberg et al., 2003). No firm conclusions can be derived from these correlations.

~2.48 Ga: An age overlap occurs between the DGS4 impact unit and onset of Huronian mafic igneous activity (2473+16/−9 Ma; Heaman, 1997), marking the onset of large-scale mafic dyke systems 2473–2446 Ma. The Matachewan-Hearst dyke systems involve volumes of at least 50,000 km^3 of basaltic magma intruding an area 250,000 km2 large (Halls and Bates, 1990). Remnants of a global ~2.50–2.42 Ga magmatic province are identified in many Archaean cratons, including the ~2.42 Ga Scourie dyke swarm (Scotland), ~2.45–2.44 Ga Karelian layered mafic intrusions, flood basalts, and dyke swarms (Finland and Russia), ~2.42 Ga Widgiemooltha dyke swarm and Jimberlana intrusion (Western Australia), dyke systems in the Vestfold Craton (Antarctica) and the ~2.42 Ga Bangalore dyke swarm (Dharwar Craton, India). The temporal coincidence of the ~2.48 Ga-old Dales (DGS4)-Kuruman asteroid mega-impact within the onset of global dyking events 2.48–2.42 Ga may be interpreted in terms of impact-induced crustal fracturing.

~ 2.030 Ga: Corresponds within error with the Vredefort impact structure dated at 2023±4 Ga (Kamo et al., 1996).

~1.870 Ga and age frequency distribution plots for the Precambrian of Western Australia (northwest Yilgarn and Gascoyne) define peaks at ~1.8 and 1.87-2.0 Ga (Nelson, 2008) (Figure 9). A partial correspondence with error with the Sudbury impact structure and its ejecta layers (1850±1 Ga, Davies, 2008) is possible.

Peaks not known to correlate with impact events include ~3336, ~1625, ~1165, ~570 and ~290 Ma (Figure 9). In the Pilbara Craton peaks at ~3.3, ~3.15, ~3.0, ~2.92 and 2.75 Ga are not known to overlap impact events. In the Yilgarn Craton peak events at ~2.75 to 2.6 Ga overlap the ~2.63 Ga Jeerinah Impact Layer toward the end.

A search for correlations between impact events and peak thermal and magmatic events is hampered by the skewed nature of the database, where only few documented well dated large impact events are known, as contrasted with thousands of accurately dated magmatic events. This imbalance likely reflects the fact that, to date, very few geologists have undertaken the "needle in the haystack" search for impact ejecta units, complicated by post-depositional corrosion and erosion of the mm-scale microkrystite spherules.

DISCUSSION: UNIFORMITARIAN MODELS AND THE ROLE OF ASTEROID IMPACTS IN CRUSTAL EVOLUTION

The increasingly detailed definition of thermal events and peak crust formation episodes through the geological record, initially by Rb-Sr isochron ages (Moorbath, 1975), and subsequently by whole grain and ion probe U-Pb zircon studies, including studies of both igneous and detrital zircons (Compston et al., 1986; Compston and Kroner, 1988; Nelson, 2008; O'Reilly et al., 2008; Valley, 2008), has progressively defined isotopic age peaks (Figures 9, 10), raising the question of the origin of the corresponding thermal events.

Isotopic age studies identify rocks crystallized or metamorphosed as early as about 4.0 Gyr, including the Acasta Gneiss, Slave Province (Iizuka et al., 2007) and in Antarctica (Harley and Kelly, 2007). These terrains include banded granite gneiss derived from metamorphosed igneous and sedimentary formations, for example in Greenland, Labrador, Slave and Superior Provinces of the Canadian Shield, Finland, South Africa, India, Western Australia and Brazil. Until the mid-20th century a long-held axiom maintained these rocks formed a primordial sial basement on which younger volcanics and sediments were deposited (Hunter, 1970; 1974; Sutton, 1971; Oversby, 1975; Bridgwater et al., 1976; Ramakrishnan et al., 1976; Moorbath, 1977; Windley, 1977; Chadwick et al., 1978; Hickman, 1981). This assumption re-emerged in the context of the discovery of pre-volcanic zircons in greenstone belts (Compston et al., 1986) and of detrital zircons up to 4.4 Gyr-old in the Narryer Terrain of the Yilgarn Craton, Western Australia (Harrison et al., 2005).

The sial basement paradigm was challenged in the early 1960's. Canadian geologists (Goodwin et al., 1974; Folinsbee et al., 1968; Card, 1990), regarded andesite volcanics and intercalated sediments infolded within Archaean gneiss as ancient analogues of circum-Pacific island arc-trench systems. Geochemical evidence and isotopic age and initial δ^{143}Nd and δ^{176}Hf data (McCulloch and Bennett, 1994; Kamber, 2007; Pietranik et al.; 2008; Valley, 2008) were increasingly interpreted in terms of plate tectonic models (Naqvi, 1976; Tarney et al., 1976; Card, 1990; Glikson, 1972, 1983, 1984, 1999; Myers, 1995; Kroner et al., 1996). To-date plate tectonic-based Archaean crustal models continue to dominate, for example on the basis of eclogite xenolith and mantle depletion studies (James and Fouch, 2002). Some authors regard rifts, marginal basins and volcanic rifted margins as the closest modern analogues to the environments of Archaean basalt-komatiite-rhyolite-dominated greenstone successions Bleeker (2002)

At the root of the debate is a fundamental question: Could the maxim "*the present is the key to the past*" be upheld? Have early Earth environments and processes significantly differed from modern plate tectonic regimes? A minority school of thought points to significant differences between Archaean greenstone belts and circum-Pacific ophiolite-turbidite accretion wedges (Glikson, 1980, Hamilton, 1998).

Engel (1966), following field studies in the Barberton mountain land, Eastern Transvaal and Swaziland (Viljoen and Viljoen, 1971; Anhaeusser, 1973), interpreted the >10 kilometer-thick sequence of pillowed Mg-rich quench basalts, peridotitic lavas and intrusive dolerite and gabbro of the `3.55 – 3.26 Ga Onverwacht Group, intercalated with thin units of quartz and feldspar-rich tuff and chert, as ancient oceanic crust. Trace element studies by Sun and Nesbitt (1978) showed the production of these Mg-rich lavas required high degrees of melting of the early mantle and high geothermal gradients.

The ubiquitous occurrence of supracrustal enclaves within granitoid gneiss, and the U-Pb and Sm-Nd evidence for sialic precursors of some of these sediments, resulted in a 'chicken and egg' impasse. Thus some of the deformed enclaves contain isotopic $^{207}Pb/^{206}Pb$ and $\delta^{143}Nd$ signatures of yet older granitoids, for example entrained zircons in volcanic and sedimentary units of the Kalgoorlie greenstone belts, Western Australia (Compston et al., 1986).

Principal differences between ancient and modern volcanic and sedimentary environments include the vertical accumulation in greenstone belts of more than 10 kilometer-thick volcanics and sediments over time spans as long as 300 million years, for example from about ~3.5 to ~3.2 Gyr in the Pilbara Craton and Kaapvaal Craton (Hickman, 2004; Hickman and Van Kranendonk, 2004; Poujol et al., 2003; Van Kranendonk et al., 2007). This contrasts with the lateral accretion of ophiolites-turbidite wedges over shorter time spans in circum-Pacific island arc-trench chains.

An important distinction between Archaean and Phanerozoic tectonic patterns is the unique structure of granite-greenstone terrains, referred to by MacGregor (1951, p.27) as 'gregarious batholiths'. As isotopic age studies progressed it has become clear that Archaean granite-greenstone systems formed through multiple geodynamic episodes, each including both volcanic and plutonic components, distinct from the more continuous accretion of circum-Pacific ophiolite-turbidite wedges (Hamilton, 1998, 2007).

Experimental petrological studies by Green (1972, 1981) suggested that, due to high geothermal gradients on the early Earth, oceanic crust was more buoyant than at present, constraining transformation of basalt into high-density garnet bearing eclogite, retarding circum Pacific-like gravity-driven subduction of oceanic crust. A variation of this concept is the low-angle subduction model by Smithies et al. (2003).

Mantle plume-based models for the origin of Archaean mafic-ultramafic volcanism (Smithies et al., 2005; Van Kranendonk et al., 2007) face the difficulty in discriminating between basaltic magmas extracted by melting of convecting upper mantle, adiabatic melting of asthenosphere triggered by deep fracturing, and deep upwelling mantle plumes. The mantle plume model remains unresolved with regard to modern volcanic systems (Hill, 1991; Griffiths and Campbell, 1991; Davies, 1999; Campbell and Davies, 2006), let alone ancient volcanic provinces.

The difficulties with Archaean models which assume extensive continental crust (Sutton, 1971, Oversby, 1975; Baragar and McGlynn, 1976; Archibald and Bettenay, 1977; Chadwick et al., 1978, Harrison et al., 2005), modified plate tectonic regimes (Tarney et al., 1976; Windley, 1977; Card et al., 1990; Krapez, 1993; Condie, 1995; Myers, 1995; de Wit, 1998; Smithies et al., 2003), mantle plume-based models (Smithies et al., 2005; Van Kranendonk et al., 2007), as highlighted by Hamilton (1998, 2003, 2007), require tests of alternative or additional factors underlying Precambrian tectono-thermal events.

The evidence indicated above for likely relationships between the 3.26–3.24 Ga multiple impacts, related unconformities and plutonic events in the Barberton greenstone belt, and contemporaneous unconformities and megabreccia units in the Pilbara Craton, as well as sharp compositional contrasts between units underlying and overlying impact fallout beds (Table 3), invites tests of potential relationships between large impacts, deep crust-lithosphere faults and onset of plate tectonic movements by further field and isotopic age investigations.

Acknowledgements

I am grateful to Alec Trendall for a constructive and meticulous review and to Arthur Hickman for helpful comments. I further wish to thank the following people for their help with the Pilbara and Kaapvaal asteroid impact studies: Gene La Berge, John Blockley, Carl Brauhart, Gary Byerly, Peter Haines, Gerta Keller, Doug Kepert, Martin Van Kranendonk, Don Lowe, Peter Morant, Franco Pirajno, Bruce Simonson, Hugh Smithies, Ian Williams, and many others.

REFERENCES

ADDISON W.D., BRUMPTON G.R., VALLINI D.A., MCNAUGHTON N.J., DAVIS D.W., KISSIN S.A., FRALICK P.W. & HAMMOND A.L. 2005. Discovery of distal ejecta from the 1850 Ma Sudbury impact event. *Geology* **33**, 193-196.

ALT A.D., SEARS J.W. & HYNDMAN D.W. 1988. Terrestrial maria: the origins of large basalt plateaus, hotspot tracks and spreading ridges. *Journal Geology* **96**, 647–662.

ALVAREZ W., ASARO F., MICHEL H.V. & ALVAREZ L.W. 1982. Iridium anomaly approximately synchronous with terminal Eocene extinctions. *Science* 216, 886–888.

ANHAEUSSER C.R. 1973. The evolution of the early Precambrian crust of southern Africa. *Philosophical Transactions Geological Society London* **A273**, 359–388.

ARCHIBALD N.J., BETTENAY L.F. 1977. Indirect evidence for tectonic reactivation of pre-greenstone basement in Western Australia. *Earth Planetary Science Letters* **33**, 370–378.

BARAGAR W.R.A., MCGLYNN J.C. 1976. Early Archaean basement in the Canadian Shield: a review of the evidence. *Geological Survey Canada Special Paper* **76–14**.

BLEEKER, W. 2002. Archaean tectonics: a review, with illustrations from the Slave craton. *Geological Society of London Special Publication*, **199,** 151-181

BOSLOUGH M.B., CHAEL E.P., TRUCANO T.G., KIPP M.E., CRAWFORD D.A. 1994. Axial focusing of impact energy in the Earth's interior: proof-of-principle tests of a new hypothesis. *Lunar Planetary Institution Contribution* **825**, 14–15.

BRIDGWATER D., COLLERSON K.D. 1976. The major petrological and geochemical characters of the 3600 m.y. Uivak gneisses from Labrador. *Contributions Mineralogy Petrology* **54**, 43–56.

BYERLY G.R., LOWE D.R. 1994. Spinels from Archaean impact spherules. *Geochimica et Cosmochimica Acta* **58**, 3469–3486.

BYERLY G.R., KRONER A., LOWE D.R., TODT W., WALSH M.M. 1995. Prolonged magmatism and time constraints for sediment deposition in the early Archaean Barberton greenstone belt: evidence from the Upper Onverwacht and Fig Tree groups. *Precambrian Research* **78**, 125–138.

BYERLY G.R., LOWE D.R., WOODEN G.L. & XIAOGANG X. 2002. A meteorite impact layer 3470 Ma from the Pilbara and Kaapvaal Cratons. *Science* **297**, 1325-1327.

CAMPBELL I.H. & DAVIES G.F. 2006. Do mantle plumes exist? *Episodes* **29**, 162-168.

CARD K.D. 1990. A review of the Superior Province of the Canadian Shield—a product of Archaean accretion. *Precambrian Research* **48**, 99–156.

CHADWICK B., RAMAKRISHNAN M., VISWANATHA M.N. & MURTHY, V.S. 1978. Structural studies in the Archaean Sargur and Dharwar supracrustal rocks of the Karnataka Craton. *Journal Geological Society of India* **29**, 531–542.

CHADWICK B. CLAEYS P. & SIMONSON B.M. 2001. New evidence for a large Palaeoproterozoic impact: spherules in a dolomite layer in the Ketilidian orogen, South Greenland, Journal of the Geological Society of London **158**, 331–340.

COLLERSON K.D., KAMBER B.S. & SCHOENBERG R. 2002. Applications of accurate, high-precision Pb isotope ratio measurement by multi-collector ICP-MS. *Chemical Geology* **188**, 65–83.

COMPSTON W., WILLIAMS I.S., CAMPBELL I.H., GRESHAM J.J. 1986. Zircon xenocrysts from the Kambalda volcanics: age constraints and direct evidence of an older continental crust below the Kambalda-Norseman greenstones. *Earth Planetary Science Letters* **76**, 299–311.

COMPSTON W. & KRONER A. 1988. Multiple zircon growth within early Archaean tonalitic gneiss from the ancient gneiss complex, Swaziland. *Earth and Planetary Science Letters* **87**, 13-28.

CONDIE K.C. 1995. Episodic ages of greenstone: a key to mantle dynamics? *Geophysical Research Letters* **22**, 2215–2218.

COURTILLOT V., JAUPART C., MANUGHETTI I., TAPPONNIER P.& BESSE J. 1999. On causal links between flood basalts and continental breakup. *Earth Planetary Research Letters* **166**, 177–196.

DAVIES G.F. 1995. Punctuated tectonic evolution of the Earth. *Earth and Planetary Science Letters* **136**,363-380.

DAVIES G.F. 1999. *Dynamic Earth: Plates, Plumes and mantle convection*. Cambridge University Press, Cambridge, 460 pp.

DAVIS D.W. 2008. Sub-million-year age resolution of Precambrian igneous events by thermal extraction–thermal ionization mass spectrometer Pb dating of zircon: Application to crystallization of the Sudbury impact melt sheet. *Geology* **36**, 383-386.

DE WIT M.J. 1998. On Archaean granites, greenstones, cratons and tectonics: does the evidence demand a verdict? *Precambrian Research* **91**, 181–226.

DIETZ R., 1964. Sudbury Structure as an Astrobleme. University of Chicago, 1964

ENGEL A.E.J. 1966. The Barberton Mountain Land: clues to the differentiation of the Earth. *University of Witwatersrand Information Circular* **27**, Johannesburg.

FOLINSBEE R.E., BAADSGAARD H., CUMMING G.L. & GREEN D.C. 1968. A very ancient island arc. *American Geophysical Union Monograph* **12**, 441–448.

FRENCH B.M., 1998. Traces of Catastrophe. *Lunar Planetary Science Contributions* **954**.

GLASS B. P. & BURNS C. A. 1988. Microkrystites. a new term for impact-produced glassy spherules containing primary crystallites. *Proceedings Lunar and Planetary Science Conference* **XVIII**, 455 – 458.

GLIKSON A.Y. 1970. Geosynclinal evolution and geochemical affinities of early Precambrian systems. *Tectonophysics* **9**, 397–433.

GLIKSON A.Y. 1971. Primitive Archaean element distribution patterns: chemical evidence and tectonic significance. *Earth Planetary Science Letters* **12**, 309–320.

GLIKSON A.Y. 1972. Early Precambrian evidence of a primitive ocean crust and island nuclei of sodic granite. *Geological Society America Bulletin* **83**, 3323–3344.

GLIKSON A.Y. 1980. Uniformitarian assumptions, plate tectonics and the Precambrian Earth. In: Kroner, A., ed., *Precambrian Plate Tectonics*. Elsevier, Amsterdam, pp. 91–104.

GLIKSON, A.Y. 1983. Geochemical, isotopic and palaeomagnetic tests of early sial-sima patterns: the Precambrian crustal enigma revisited. *Geological Society America Memoir* **161**, 95-118.

GLIKSON A.Y. 1984. Significance of early Archaean mafic- ultramafic xenolith patterns. In: Kroner, A., Goodwin, A.M., Hanson, G.N., eds., *Archaean Geochemistry*. Springer-Verlag, Berlin, pp. 263–280.

GLIKSON A.Y. 1993. Asteroids and early Precambrian crustal evolution. *Earth Science Reviews* **35**, 285–319.

GLIKSON A.Y. 1994. Archaean spherule beds: impact or terrestrial origin? *Earth Planetary Science Letters* **26**, 493–496.

GLIKSON A.Y. 1996. Mega-impacts and mantle melting episodes: tests of possible correlations. *Australian Geological Survey Organization Journal Australia Geology and Geophysics* **16**, 587–608.

GLIKSON A.Y. 1999. Oceanic mega-impacts and crustal evolution. *Geology* **27**, 341–387.

GLIKSON A.Y. 2004. Early Precambrian asteroid impact-triggered tsunami: excavated seabed, debris flows, exotic boulders, and turbulence features associated with 3.472 Ga-old asteroid impact fallout units, Pilbara Craton, Western Australia. *Astrobiology* **4**, 5–19.

GLIKSON A.Y. 2005A. Geochemical and isotopic signatures of Archaean to Palaeoproterozoic extraterrestrial impact ejecta/fallout units. *Australian Journal Earth Science*, **52**,785-798.

GLIKSON, A.Y., 2005B. Geochemical signatures of Archean to Early Proterozoic maria-scale oceanic impact basins. *Geology*, **133**, 125-128.

GLIKSON A.Y. 2006. Asteroid impact ejecta units overlain by iron-rich sediments in 3.5–2.4 Ga terrains, Pilbara and Kaapvaal cratons: Accidental or cause–effect relationships? *Earth Planetary Science Letters* **246**, 149-160

GLIKSON A.Y. 2007a. Early Archaean asteroid impacts on Earth: stratigraphic and isotopic age correlations and possible geodynamic consequences. *Earth's Oldest Rocks*, M.J. Van Kranendonk, Smithies, H.R., Bennett, V.C., eds., *Development in Precambrian Geology* **15**, Elsevier, 1087-1103.

GLIKSON, A.Y. 2007b. Siderophile element patterns, PGE nuggets and vapour condensation effects in Ni-rich quench chromite-bearing microkrystite spherules, 3.24 Ga S3 impact unit, Barberton greenstone belt, Kaapvaal Craton, South Africa. *Earth and Planetary Science Letters* **253**, 1-16.

GLIKSON A.Y. 2008. Field evidence of Eros-scale asteroids and impact-forcing of Precambrian geodynamic episodes, Kaapvaal (South Africa) and Pilbara (Western Australia) Cratons. *Earth Planetary Science Letters* **267**, 558-570

GLIKSON A.Y. & SHERATON J.W. 1972. Early Precambrian trondhjemitic suites in Western Australia and northwestern Scotland and the geochemical evolution of shields. *Earth Planetary Science Letters* **17**, 227–242.

GLIKSON A.Y., ALLEN C. & VICKERS J. 2004. Multiple 3.47-Ga-old asteroid impact fallout units, Pilbara Craton, Western Australia. *Earth Planetary Science Letters* **221**, 383–396.

GLIKSON, A.Y., & ALLEN, C., 2004. Iridium anomalies and fractionated siderophile element patterns in impact ejecta, Brockman Iron Formation, Hamersley Basin, Western Australia: evidence for a major asteroid impact in simatic crustal regions of the early Proterozoic earth. Earth Planet. Sci. Lett. 220, 247–264

GLIKSON A.Y. & VICKERS J. 2005. The 3.26–3.24 Ga Barberton asteroid impact cluster: Tests of tectonic and magmatic consequences, Pilbara Craton, Western Australia. *Earth Planetary Science Letters* **241**, 11-20.

GLIKSON A.Y. & VICKERS J. 2006. Asteroid mega-impacts and Precambrian banded iron formations: 2.63 Ga and 2.56 Ga impact ejecta/fallout at the base of BIF/argillite units, Hamersley Basin, Pilbara Craton, Western Australia. *Earth Planetary Science Letters* **254**, 214-226.

GOODWIN A.M. 1974. Precambrian belts, plumes and shield development. *American Journal* of Science **274**, 987-1028.

GREEN D.H. 1972. Archaean greenstone belts may include terrestrial equivalents of lunar maria? *Earth Planetary Science Letters* **15**, 263–270.

GREEN D.H. 1981. Petrogenesis of Archaean ultramafic magmas and implications for Archaean tectonics. In: Kroner A., ed., *Precambrian Plate Tectonics*. Elsevier, Amsterdam, pp. 469–489.

GRIEVE R.A.F. 1980. Impact bombardment and its role in proto-continental growth of the early Earth. *Precambrian Research* **10**, 217–248.

GRIEVE R.A.F. & DENCE M.R. 1979. The terrestrial cratering record: II. The crater production rate. *Icarus* **38**, 230–242.

GRIEVE R.A.F. & SHOEMAKER E.M. 1994. The Record of Past Impacts on Earth. The University of Arizona Press, Tucson, Arizona.

GRIEVE R.A.F. & PESONEN L.J. 1996. Terrestrial impact craters: their spatial and temporal distribution and impacting bodies. *Earth, Moon and Planets* **72**, 357–376.

GRIEVE R.A.F. & PILKINGTON M. 1996. The signature of terrestrial impacts. *Australian Geological Survey organization Journal Australian Geology and Geophysics* **16**, 399–420.

GRIFFITHS R.W., CAMPBELL I.H. 1991. Interaction of mantle plume heads with the Earth’s surface and onset of small scale convection. *Journal Geophysical Research* **96**, 18295–18310.

HALL H.C. & BATES M.P. 1990. The evolution of the 2.45 Ga Matachewan dyke swarm. In: Parker A.J. et al., eds, *Mafic Dykes and Emplacement Mechanisms*. Balkema, Canada, pp. 237–249.

HARRISON T.M., BLICHERT-TOFT J., MULLER W., ALBAREDE F., HOLDEN P. & MOJZSIS S.J. 2005. Heterogeneous Hadean hafnium; Evidence of continental crust by 4.4–4.5 Ga. *Science* **310**, 1947–1950,

HAMILTON W.B. 1998. Archaean magmatism and deformation were not products of plate tectonics. *Precambrian Research* **91**, 143–179.

HAMILTON W.B., 2003. An alternative Earth. *GSA Today* **13**, 4-12.

HAMILTON W.B., 2007. Comment on "A Vestige of Earth's Oldest Ophiolite". *Science* **318**, 746.

HARLEY S.L. & KELLY N.M. 2007. Ancient Antarctica: The Archaean of the East Antarctic shield. In: *Earth's Oldest Rocks*, Van Kranendonk, M.J., Smithies, H.R., Bennett, V.C., eds., *Development in Precambrian Geology*, **15**, Elsevier, 149-186

HEAMAN L.M. 1997. Global mafic magmatism at 2.45 Ga: remnants of an ancient large igneous province? *Geology* **25**, 299–302.

HICKMAN A.J. 1981. Crustal evolution of the Pilbara Block, Western Australia. *Geological Society Australia Special Publication* **7**, 57–69.

HICKMAN A.J. 2004. Two contrasting granite-greenstone terrains in the Pilbara Craton, Australia: evidence for vertical and horizontal tectonic regimes prior to 2900 Ma. *Precambrian Research* **131**, 153-172.

HICKMAN A.H. & VAN KRANENDDONK M.J. 2004. Diapiric processes in the formation of the Archaean continental crust, east Pilbara granite-greenstone terrain, Australia. In: ERIKSSON et al., eds., *The Precambrian Earth*: *Tempos and Events.* Elsevier, Amsterdam, pp. 54-75.

HILL R.I. 1991. Starting plumes and continental breakup. *Earth Planetary Science Letters* **104**, 398–416.

HUGHS H.G., APP F.N. & MCGETCHIN T.N. 1977. Global seismic effects of basin-forming impacts. *Physics of the Earth and Planetary Interiors* **15**, 251–263.

HUNTER D.R. 1970. The ancient gneiss complex in Swaziland. *Transactions Geological Society Africa* **73**, 105–107.

HUNTER D.R. 1974. Crustal development in the Kaapvaal Craton: part 1—the Archaean. *Precambrian Research* **1**, 259–294.

IIZUKA T., KOMIYA T. & MARUYAMA S., 2007. The early Archaean Acasta gneiss complex: geological, geochronological and isotopic studies and implications for early crustal evolution. In: *Earth's Oldest Rocks*, Van Kranendonk, M.J., Smithies, H.R., Bennett, V.C., eds., *Development in Precambrian Geology*, **15**, 127-148.

JAMES D. E. & FOUCH, M. J. 2002. Formation and evolution of Archaean cratons: insights from southern Africa. *Geological Society of London Special Publication*, **199**, 91 - 103

JONES A.G. 1987. Are impact-generated lower crustal faults observable? *Earth Planetary Science Letters* **85**, 248–252.

KAMBER B.S. 2007. The enigma of the terrestrial protocrust: evidence for its former existence and importance of its complete disappearance. In: *Earth's Oldest Rocks*, Van Kranendonk, M.J., Smithies, H.R., Bennett, V.C., eds., *Development in Precambrian Geology*, **15**, 75-90.

KAMO S.L., REIMOLD W.U., KROUGH T.E. & Colliston W.P. 1996. A 2.023 Ga age for the Vredefort impact event and a first report of shock metamorphosed zircons in pseudotachylitic breccias and granophyre. *Earth and Planetary Science Letters* **144**, 369-387.

KRAPEZ B. 1993. Sequence stratigraphy of the Archaean supracrustal belts of the Pilbara Block, Western Australia. *Precambrian Research* **60**, 1–45.

KYTE F.T., ZHOU L. & LOWE D.R. 1992. Noble metal abundances in an early Archaean impact deposit. *Geochimica Cosmochimica Acta* **56**, 1365–1372.

LOWE D.R. 1980. Stromatolites 3800 Myr old from the Archaean of Western Australia. *Nature* **284**, 441-443.

LOWE D.R. & BYERLY G.R. 1986. Early Archaean silicate spherules of probable impact origin, South Africa and Western Australia. *Geology* **14**, 83–86.

LOWE D.R., BYERLY G.R., ASARO F. & KYTE F.T. 1989. Geological and geochemical record of 3400 Million years old terrestrial meteorite impacts. *Science* **245**, 959–962.

LOWE D. R., BYERLY G. R., KYTE F.T., SHUKLOYUKOV A., ASARO F. & KRULL A. 2003. Spherule beds 3.47 – 3.34 Ga-old in the Barberton greenstone belt, South Africa: a record of large meteorite impacts and their influence on early crustal and biological evolution. *Astrobiology* **3**, 7–48.

MACGREGOR, A.M. 1952. Some milestones in the Precambrian of southern Rhodesia. Anniversary address by President. Proceedings of the Geological Society of South Africa, IIV, xxvii-lxxiv.

MARY GEE M.A. & SWAGER C. 2008. Late Archaean volcanic arcs and their accretionary history, Eastern Goldfields Superterrane: Plate tectonic models inferred from tectonostratigraphic analysis. *Precambrian Research* **161**, 1-4.

MARVIN U.B. 1990. Impact and its revolutionary implications for geology. *Geological Society of America Special Paper* **247**, 147–154.

MCCULLOCH M.T. & Bennett V.C. 1994. Progressive growth of the Earth's continental crust and depleted mantle: geochemical constraints. *Geochimica Cosmochimica Acta* **58**, 4717–4738.

MELOSH H.J. & VICKERY A.M. 1991. Melt droplet formation in energetic impact events. *Nature* **350**, 494–497.

MORGAN, W.J. 1981. Hotspot tracks and the opening of the Atlantic and Indian oceans. In: *The Sea*, Emiliani C., ed., Wiley Interscience, New York, Vol. 7, pp. 443–487.

MOORBATH S. 1975. Evolution of Precambrian crust from Strontium isotopic evidence. *Nature* **254**, 395-398.

MOORBATH S. 1977. Ages, isotopes and the evolution of the Precambrian continental crust. *Chemical Geology* **20**, 151-187.

MOJZSIS S.J. & HARRISON T.M. 2002. Establishment of a 3.83-Ga magmatic age for the Akilia tonalite, southern West Greenland. *Earth and Planetary Science Letters* **202**, 563-576

MUKASA S.B., WILSON A.H. & CARLSON R.W. 1998. A multi-element geochronological study of the Great Dyke, Zimbabwe: significance of the robust and reset ages. *Earth Planetary Science Letters* **164**, 353–369.

MYERS J.S. 1995. The generation and assembly of an Archaean supercontinents: evidence from the Yilgarn craton, Western Australia. *Geological Society London Special Publication* **95**, 1439–1454.

NAQVI S.M. 1976. Physical-chemical conditions during the Archaean as indicated by Dharwar geochemistry. In: *Early History of the Earth*, Windley B.F., ed., John Wiley & Sons, London, pp. 289–298.

NELSON D.R. 2008. Geochronology of the Archaean of Australia. *Australian Journal of Earth Sciences* **55**, 779-793.

NUTMAN A.P., FRIEND C.R.L., HORIE K. & HIDAKA H. 2007. The Itsaq gneiss complex of southwestern Greenland and the construction of Eoarchaen crust at convergent plate boundaries. n: *Earth's Oldest Rocks*, Van Kranendonk, M.J., Smithies, H.R., Bennett, V.C., eds., *Development in Precambrian Geology*, **15**, 187-218

OBERBECK V.R., MARSHALL J.R. & AGGARVAL H. 1992. Impacts, tillites and the breakdown of Gondwanaland. *Journal Geology* **101**, 1–19.

O'REILLY S.Y., GRIFFIN W.L., PEARSON N.J., JACKSON S.E., BELOUSOVA E.A., ALARD O. & SAEED A. 2008. Taking the pulse of the Earth. *Australian Journal of Earth Science* **55**, 983-996.

OVERSBY V.M. 1975. Lead isotopic systematics and ages of Archaean acid intrusives in the Kalgoorlie-Norseman area, Western Australia. *Geochimica Cosmochimica Acta* **40**, 1107–1125.

PIETRANIK A.B., HAWKESWORTH C.J., STOREY C.D., KEMP T.I., SIRCOMBE K.N., WHITEHOUSE M.J. & BLEEKER W. 2008. Episodic, mafic crust formation from 4.5 to 2.8 Ga: New evidence from detrital zircons, Slave craton, Canada. *Geology* **36**, 875–878.

POUJOL M., ROBB L.J., ANHAEUSSER C.R. & GERICKE B. 2003. A review of the geochronological constraints on the evolution of the Kaapvaal Craton, South Africa. *Precambrian Research* **127**, 181-213.

RAMAKRISHNAN, M., VISWANATHA, N.M. & SWAMI NATH, J. 1976. Basement-cover rlations in peninsular gneiss with high grade schists and greenstone belts of southern Karnataka. *Journal of the Geological Society of India* **17**, 97-111.RASMUSSEN B. & KOEBERL C. 2004. Iridium anomalies and shocked quartz in a Late Archean spherule layer from the Pilbara Craton: New evidence for a major asteroid impact at 2.63 Ga. *Geology* **32**, 1029–1032.

RASMUSSEN B., BLAKE T.S. & FLETCHER I.R. 2005, U-Pb zircon age constraints on the Hamersley spherule beds: Evidence for a single 2.63 Ga Jeerinah-Carawine impact ejecta layer. *Geology* **33**, 725–728.

RICHARDS M.A., DUNCAN R.A. & COURTILLOT V., 1989. Flood basalts and hot spot tracks: plume heads and tails. *Science* **246**, 103–107.

RYDER G. 1990. Lunar samples, lunar accretion and the early bombardment of the Moon. *Eos* **71**, 313–322.

RYDER G. 1991. Accretion and bombardment in the Earth-Moon system: the Lunar record. *Lunar Planetary Institute Contribution* **746**, 42–43.

RYDER G. 1997. Coincidence in the time of the Imbrium Basin impact and Apollo 15 Kreep volcanic series: impact induced melting? *Lunar Planetary Institute Contribution* **790**, 61–62.

SCHOENBERG R., NÄGLER T.H.F., GNOS E., KRAMERS J.D. & KAMBER B.S., 2003. The source of the great dyke, Zimbabwe, and its tectonic significance: evidence from Re–Os isotopes. *The Journal of Geology* **111**, 565–578.

SHOEMAKER E.M. & SHOEMAKER C.S. 1996. The Proterozoic impact record of Australia. Australian *Geological Survey Organization Journal Australia Geology Geophysics* **16**, 379–398.

SHUKLOYUKOV A., KYTE, F.T., LUGMAIR, G.W., LOWE, D.R., BYERLY, G.R. 2000. The oldest impact deposits on earth — First confirmation of an extraterrestrial component In: *Impacts and the Early Earth. Editor: Iain Gilmour, Christian Koeberl, Lecture Notes in Earth Science* **91**, 99-115

SIMONSON B.M. 1992. Geological evidence for an early Precambrian microtektite strewn field in the Hamersley Basin of Western Australia. *Geological Society America Bulletin* **104**, 829–839.

SIMONSON B.M. & HASSLER, S.W. 1997. Revised correlations in the early Precambrian Hamersley Basin based on a horizon of resedimented impact spherules. *Australian Journal Earth Science* **44**, 37–48.

SIMONSON B.M. & GLASS B.P. 2004. Spherule layers — records of ancient impacts. *Annual Review Earth Planetary Science* **32**, 329–361.

SIMONSON B.M., DAVIES D. & HASSLER S.W., 2000. Discovery of a layer of probable impact melt spherules in the late Archean Jeerinah Formation, Fortescue Group, Western Australia. *Australian Journal Earth Science* **47**, 315–325.

SIMONSON B.M., SUMNER D.Y., BEUKES, N.J., JOHNSON, S., GUTZMER, J. 2009.. Correlating multiple Neoarchean–Paleoproterozoic impact spherule layers between South Africa and Western Australia. *Precambrian Research* **169**, 100-111.

SLEEP N.H. 2008. Plate tectonics through time, In: *Evolution of the Earth*, Stevenson, D., ed., *Treatise on Geophysic* **9**, 145–169.

SMITHIES R.H., CHAMPION D.C. & CASSIDY K.F. 2003. Formation of Earth's early Archaean continental crust. *Precambrian Research* **127**, 89–101.

SMITHIES R.H., VAN KRANENDDONK M.J. & CHAMPION D.C. 2005. It started with a plume: Early Archaean basaltic protocontinental crust. *Earth and Planetary Science Letters* **238**, 284-297.

SUN S. & NESBITT R.W. 1978. Petrogenesis of Archaean ultrabasic and basic volcanics: evidence from rare earth elements, *Contributions Mineralogy Petrology* **65**, 301-325, 1978

SUTTON J. 1971. Some developments in the crust. *Geological Society Australia Special Publication* **3**, 1–10.

TARNEY J., DALZIEL I.W.D. & DE WIT M.J., 1976. Marginal Basin 'Rocas Verdes' complex from south Chile: a model for Archaean greenstone belt formation. In: *The Early History of the Earth*, Windley B.F. ed., John Wiley & Sons, New York, pp. 131–146.

TRENDALL A.F., COMPSTON W., NELSON D.R., DELAETER J.R., BENNETT V.C., 2004. SHRIMP zircon ages constraining the depositional chronology of the Hamersley Group, Western Australia. *Australian Journal Earth Science* **51**, 621–644.

VALLEY J.W. 2008. The origin of habitats. *Geology* **36**, 911-912.

VAN KRANENDONK M.J. & MORANT P. 1998. Revised Archaean stratigraphy of the North Shaw 1:100 000 sheet, Pilbara Craton. *Geological Survey Western Australia Annual Report for 1997*, pp. 55–62.

VAN KRANENDONK M.J. 2007. Tectonics of the early Earth. In: *Earth's Oldest Rocks*, Van Kranendonk, M.J., Smithies, H.R., Bennett, V.C., eds., *Development in Precambrian Geology*, **15**, 1105-1116.

VAN KRANENDONK, M.J., SMITHIES, R.H., HICKMAN, A.H. & CHAMPION, D.C., 2007. Paleoarchaean development of a continental nucleus: the east Pilbara terrain of the Pilbara Craton, Western Australia. In: *Earth's Oldest Rocks*, Van Kranendonk, M.J., Smithies, H.R., Bennett, V.C., eds., *Development in Precambrian Geology*, **15**, 307-338.

VILOEN R.P. & VILJOEN M.J. 1971. The geological and geochemical evolution of the Onverwacht Group in the Barberton Mountain Land, South Africa. *Geological Society Australia Special Publication* **3**, 133–151.

WINDLEY B.F. 1977. *The Evolving Continents.* John Wiley & Sons, London.

FIGURES

Fig. 1

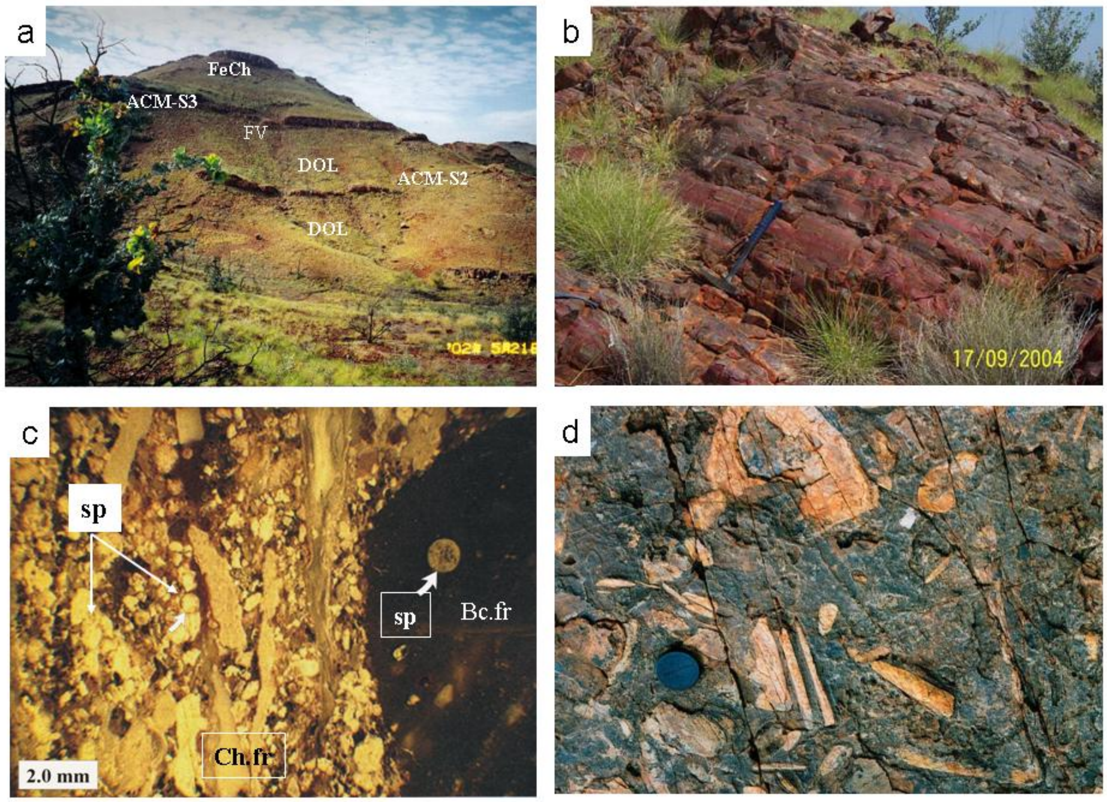

Figure 1

Pilbara ~3.47 impact ejecta units.

~3.47 Ga impact fallout units, Antarctic Chert Member, base Apex Basalt, North Pole dome, Pilbara Craton.

A. Type locality of the ~3.47 Ga impact unit, Antarctic Chert Member (ACM), base Apex Basalt, north of Miralga Creek. North Pole dome, Abbreviations: ACM-S3, spherule-bearing diamictite; ACM-S2, spherule-bearing chert and arenite; FV – felsic volcanics or sill; DOL - dolerite; FeCh – jaspilite. Miralga Creek: 21°08’37.41”S/119°.28’52.12”E.
B. Jaspilite at the top of the ACM overlying the impact fallout unit. Miralga Creek: 21°04’21.06”S/119°2803.57”E.
C. Microkrystite-bearing chert diamictite of impact unit ACM-S3. Slide AG-MC-01.
D. Microkrystite spherule-bearing breccia-conglomerate of ACM-S2. Miralga Creek: 21°08’37.41”S/119°.28’52.12”E.
E.

Fig. 2

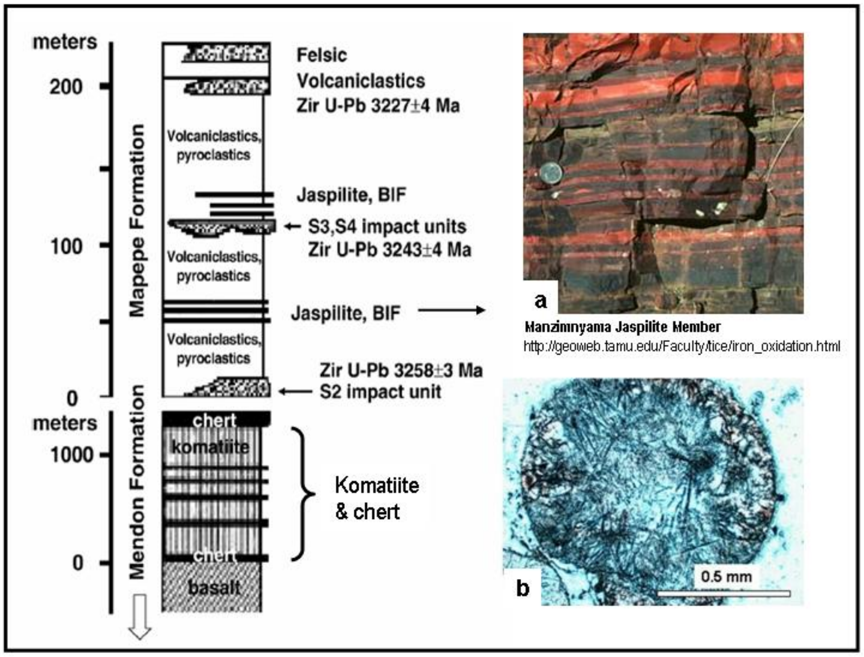

Figure 2

Barberton ~3.26 – 3.24 impact ejecta units.

Barberton greenstone belt: Simplified columnar section of the contact between the Mendon Formation komatiite-basalt-chert unit, overlying S2, S3 and S4 impact ejecta units, volcaniclastic sediments, pyroclastics and jaspilite (after Lowe et al., 2003). Note the variation in scale.

A. Banded chert and jasper of the Manzimnyama Jaspilite Member.

B. Impact spherule of the S3 spherule unit, showing microlites of chlorite after pyroxene. Slide AG_BGB-S3-01.

Fig 3

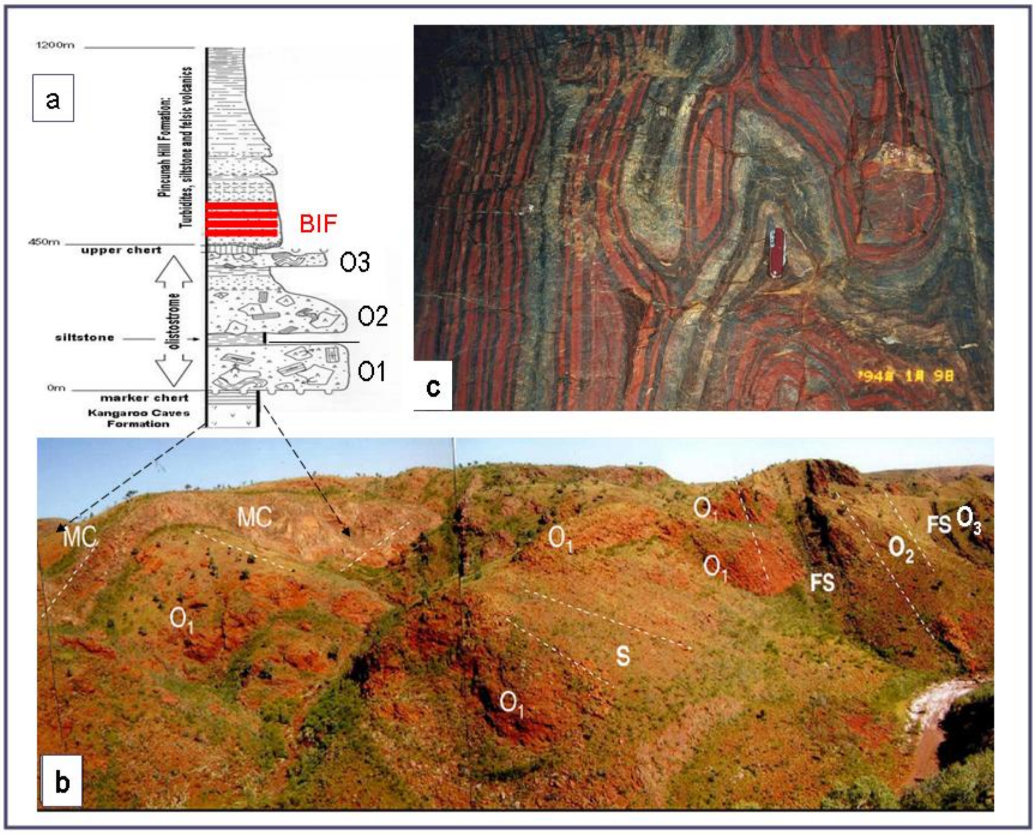

Figure 3

Pilbara equivalents of the Barberton ~3.24 Ga impact level.

A. Schematic columnar section of the transition from volcanics of the Sulphur Springs Group (dacite of Kangaroo Caves Formation; 3235±3 Ma), capped by Marker Chert, overlain by 3 olistostrome units separated by ferruginous shale. $0_{1\text{-}3}$ – Olistostrome units 1 – 3

B. Large blocks of chert, siltstone and siliceous volcanics in the Sulphur Springs area, central Pilbara Block, occupying a stratigraphic position similar to that of 3.24 Gyr impact fallout units in the Barberton Mountain land, South Africa, signifying major faulting near-contemporaneous with asteroid impacts. $0_{1\text{-}3}$ – Olistostrome units 1 – 3; S – shale; FS – ferruginous shale; MC – Marker Chert. Looking west from Sulphur Springs Creek: 119°12'18.32"E/21°08'47.01S.

C. Jaspilite and banded iron formation of the ~3.2 Ga Paddy Market Formation, Soanesville Group, stratigraphically above the stromatolite. Coppin Gap:120°07'06.08"E/20°52'59.31"S.

Fig. 4

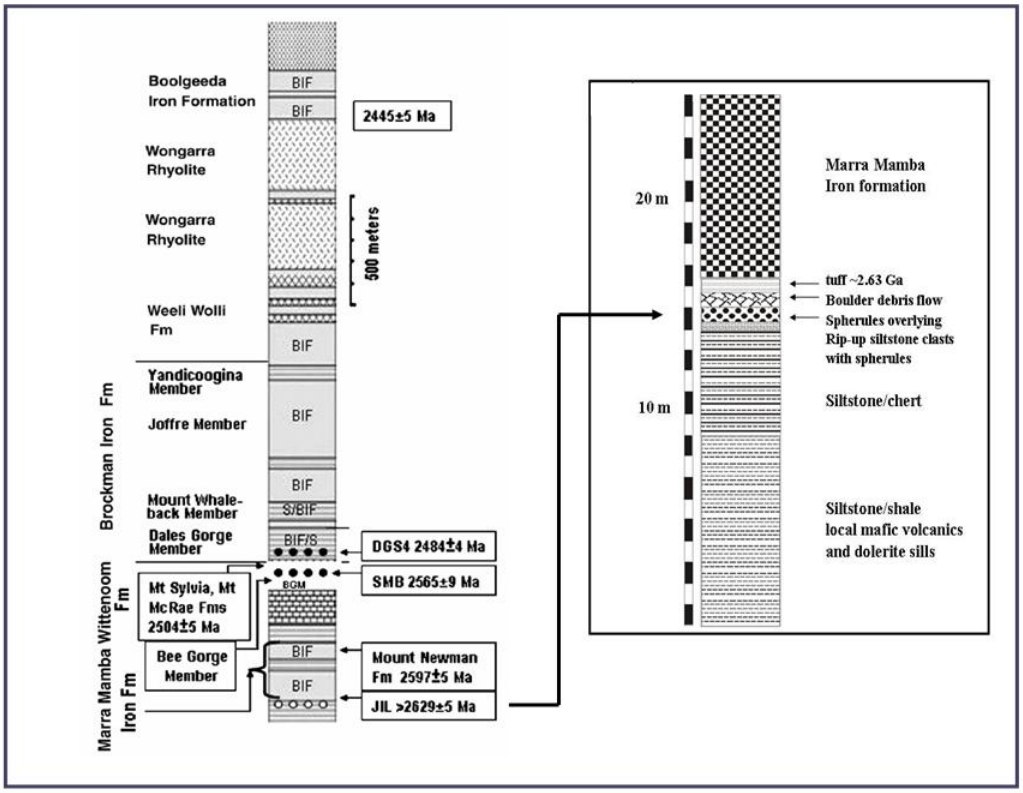

Figure 4

Schematic stratigraphic column of Hamersley Basin stratigraphy and ages (Isotopic ages after Trendall et al., 2004). Right: stratigraphic position of the ~2.63 Ga Jeerinah Impact Layer.

Fig. 5

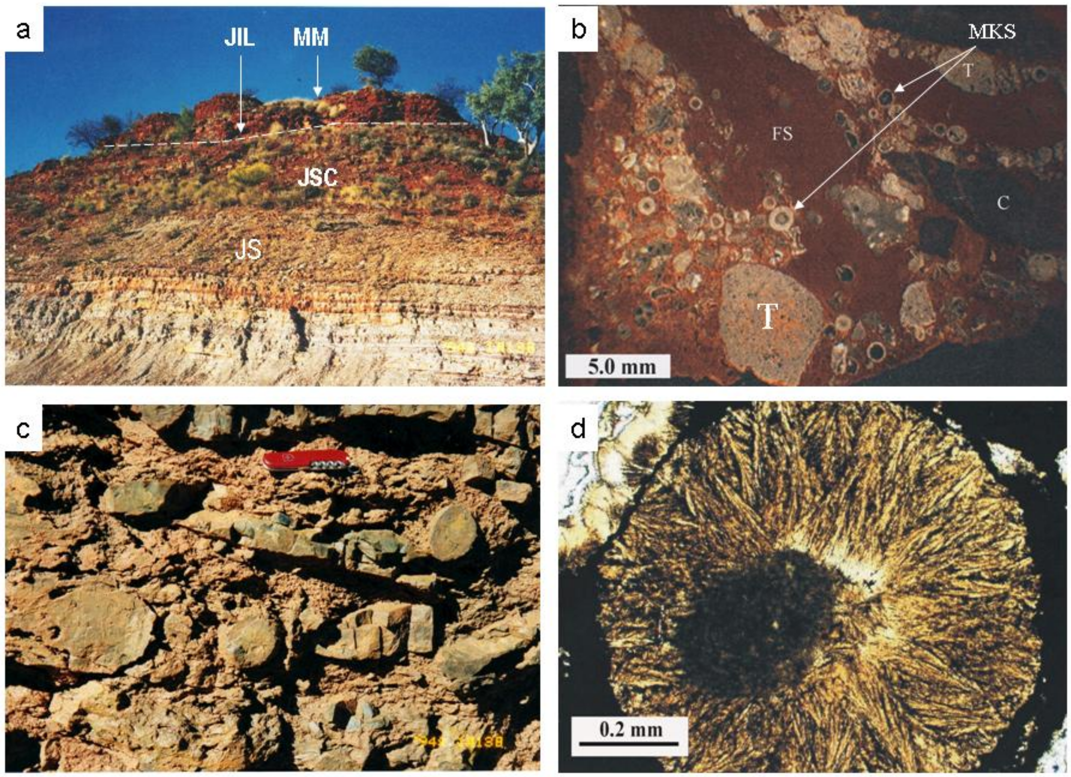

Figure 5

~2.63 Ga Jeerinah Impact Layer.

A. Type locality of the Jeerinah Impact Layer (JIL) (Simonson et al., 2000) at Hesta Railway Siding, central Pilbara. JS – Jeerinah Shale; JSC – JS shale and chert; MM – Marra Mamba Iron Formation. Hesta siding: 22°11’18.06”S/119°01’48.77″

B. Basal breccia of JIL consisting of fragments of ferruginous shale, microkrystite spherules (MKS) and tektites (T). Slide AG-JIL-HES-01

C. Debris flow consisting of fragments and boulders of chert, overlying JIL. Hesta siding: 22°11’18.06”S/119°01’48.77″

D. Microkrystite spherule consisting of inward-radiating fans of quenched potassium feldspar crystallites enveloping an offset core of carbonate and chlorite, set in fragmental arenite matrix. The Iridium-rich spherule condensed from impact-released vapor. Slide AG-JIL-HES-02

Fig. 6

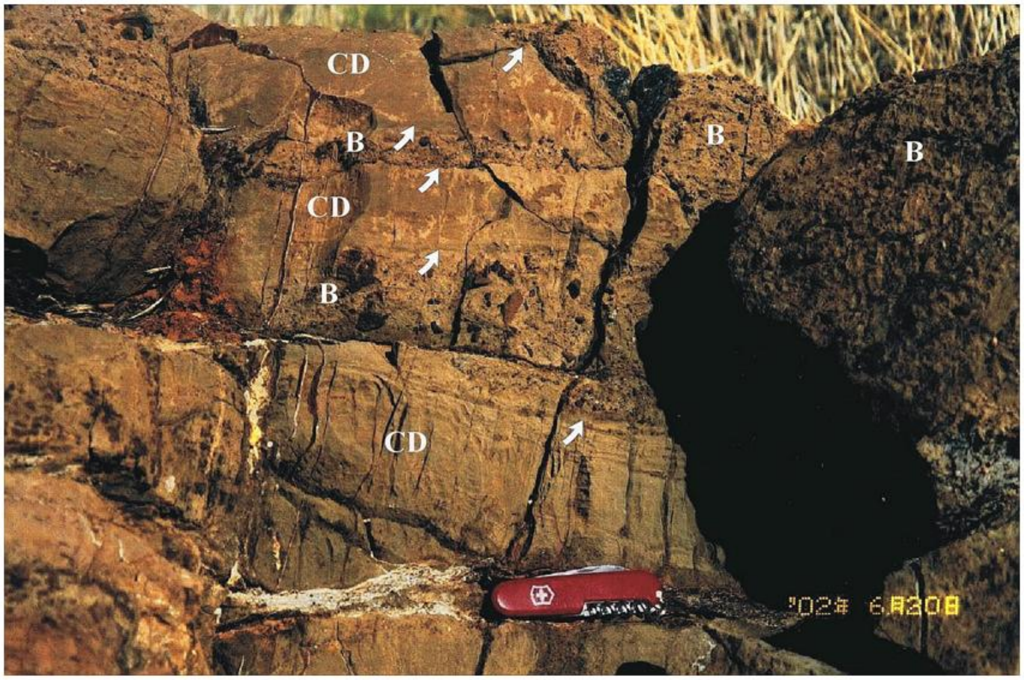

Figure 6

Concordant, subconcordant and vein breccia (B) injected into Carawine Dolomite (CD) carbonate south of Woodie-Woodie, the East Hamersley Basin, Pilbara Craton. The matrix of the fragmented breccia contains microkrystite impact spherules. South of Woodie Woodie manganese mines: 21^{0}46'35.04"S/121°13'59.75"E

Fig. 7

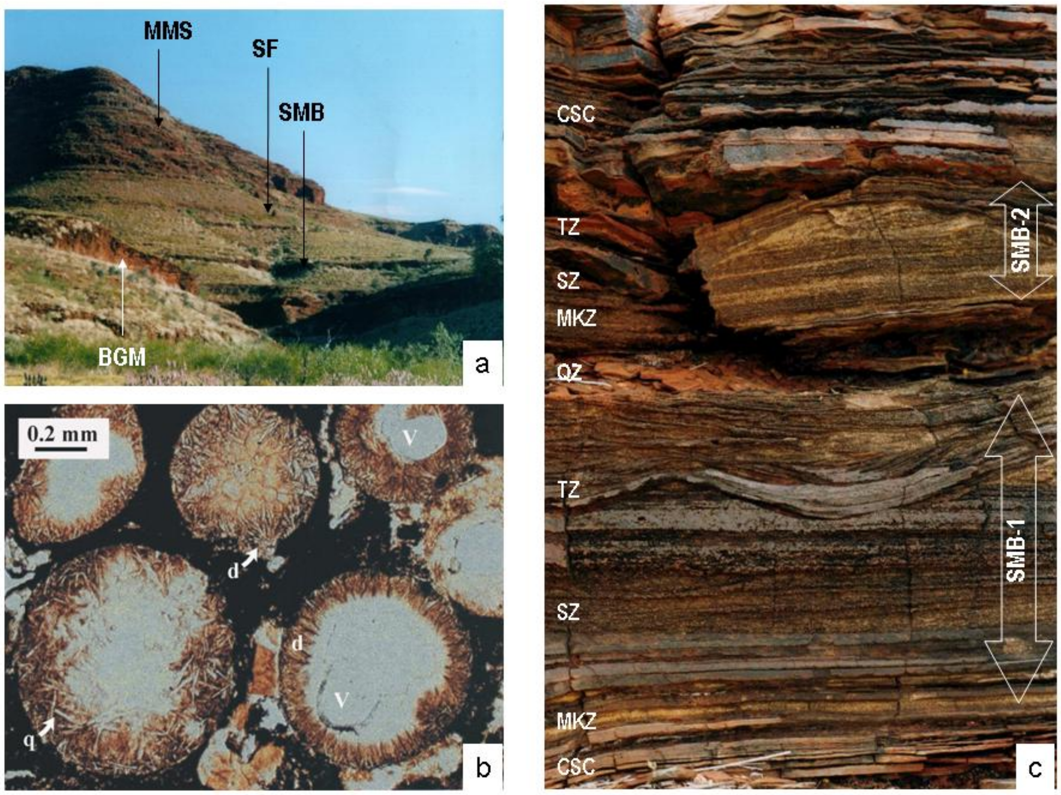

Figure 7

~2.56 Ga Spherule Marker Bed (SMB), Hamersley Basin.

A. Bee Gorge section, showing the SMB horizon above the Bee Gorge carbonate-shale member (BGM) of the Wittenoom Formation, below the Sylvia Formation (SF) (ferruginous shale and chert), below the Mount McRae ferruginous shale and banded iron formation (MMS). Bee Gorge: 22°13′20.83″S/118°15′47.14″E

B. Microkrystite spherules of the SMB. q – quench K-feldspar crystallites; V – outline of vesicle; d –devitrification features of radiating K-feldspar crystallites. Slide AG-MUN-SMB-01.

C. Munjina Gorge section of the SMB showing two impact cycles, SMB-1 and SMB-2, overlain and underlain by carbonate, siltstone, and chert (CSC). Each cycle includes a basal layer or series of lenses of microkrystite spherules (MKZ) overlain by rhythmic turbidites (seismic zone, SZ), overlain by a cross rippled tsunami zone (TZ). The two cycles are separated by a stratigraphically consistent layer of silicified black siltstone denoted as a "Quiet Zone" (QZ). Munjina Gorge: 22°24′31.43″S/118°41′18.47″E

Fig. 8

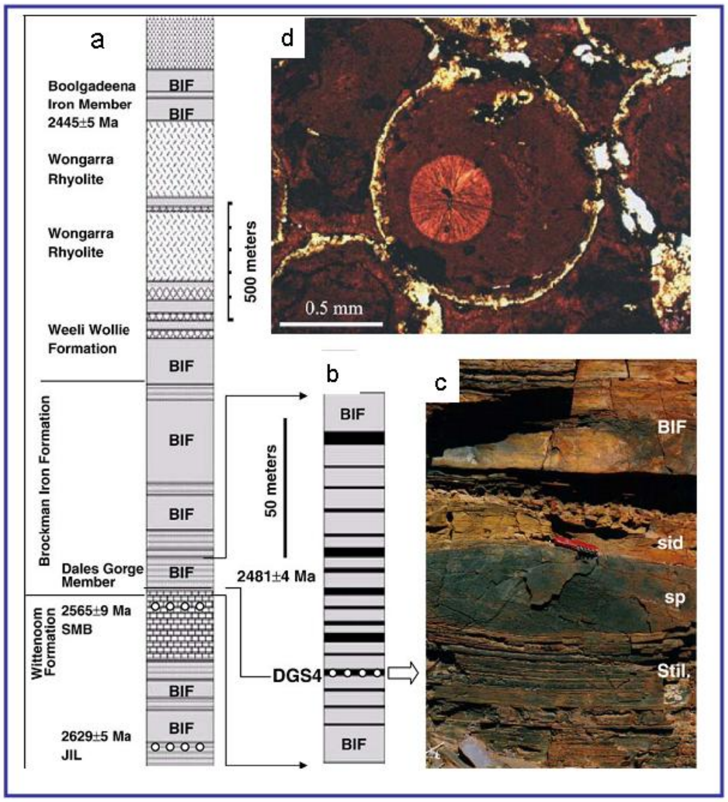

Figure 8

Impact ejecta of the ~2.48 Ga Shale Macroband of the Dales Gorge Member, Brockman Iron formation.

A. Schematic columnar diagrams showing main units of the Hamersley Group and U–Pb zircon isotopic ages (after Trendall et al., 2004). JIL – Jeerinah Impact Layer; SMB – Spherule Marker Bed.

B. Banded iron macrobands and shale macrobands of the Dales Gorge Member, showing the DGS4.

C. Outcrop of impact spherule-bearing band (sp) at the top of DGS4, overlying finely laminated stilpnomelane-dominated tuff/sediment bands (Stil.), and underlying siderite-rich siltstone band (sid) and banded iron-formation (BIF). Dales Gorge: 22°28′55.2″S/118°33′14.34″E

D. Stilpnomelane-dominated impact spherules (microkrystites) rimmed by thin light feldspar rims and cored by radiating centrally offset vesicle of stilpnomelane. Slide AG-DGS4-01

Fig. 9

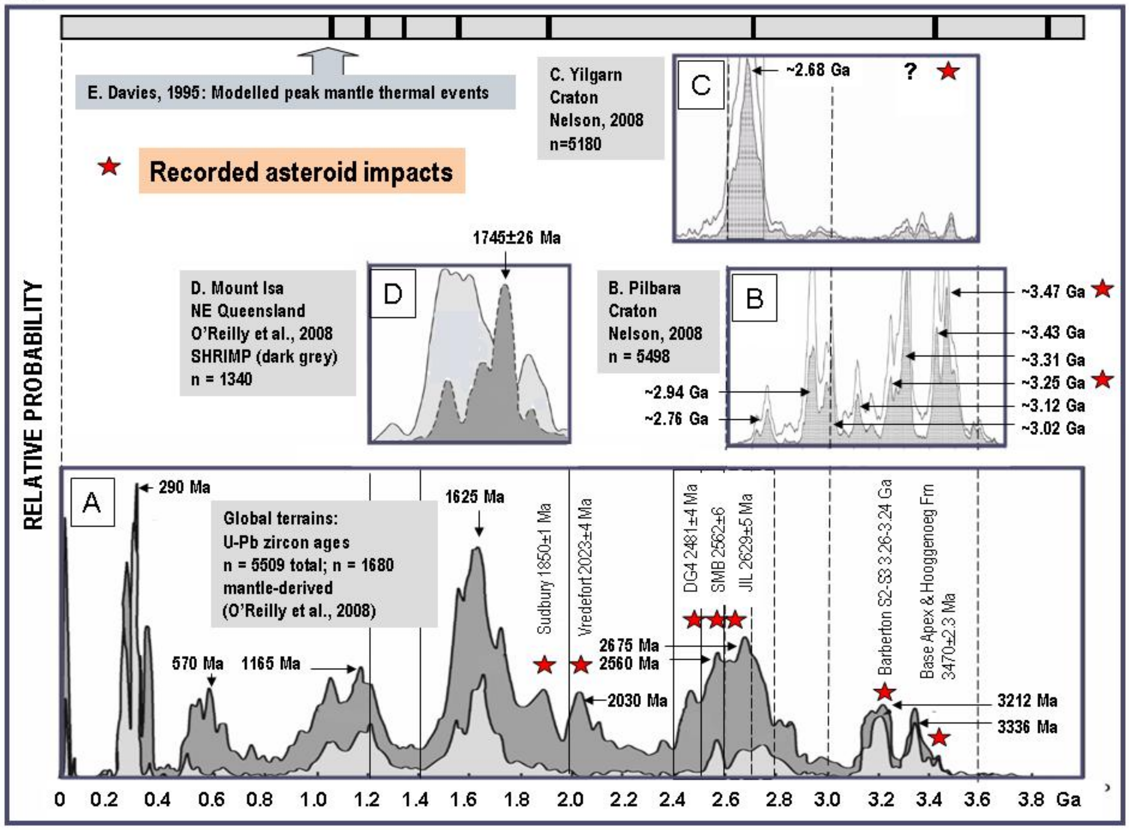

Figure 9

Isotopic U-Pb zircon age frequency distribution (relative probability) diagrams

A. Global (after O'Reilly et al., 2008);
B. Pilbara Craton, Western Australia (after Nelson, 2008);
C. Yilgarn Craton, Western Australia (after Nelson, 2008);
D. Northwest Queensland (after Nelson, 2008).
E. Model mantle thermal events (Davies, 1995).

Stars represent recorded large asteroid impacts. Impact ages located above stars; histogram peaks – pointed by horizontal arrows.

Fig. 10

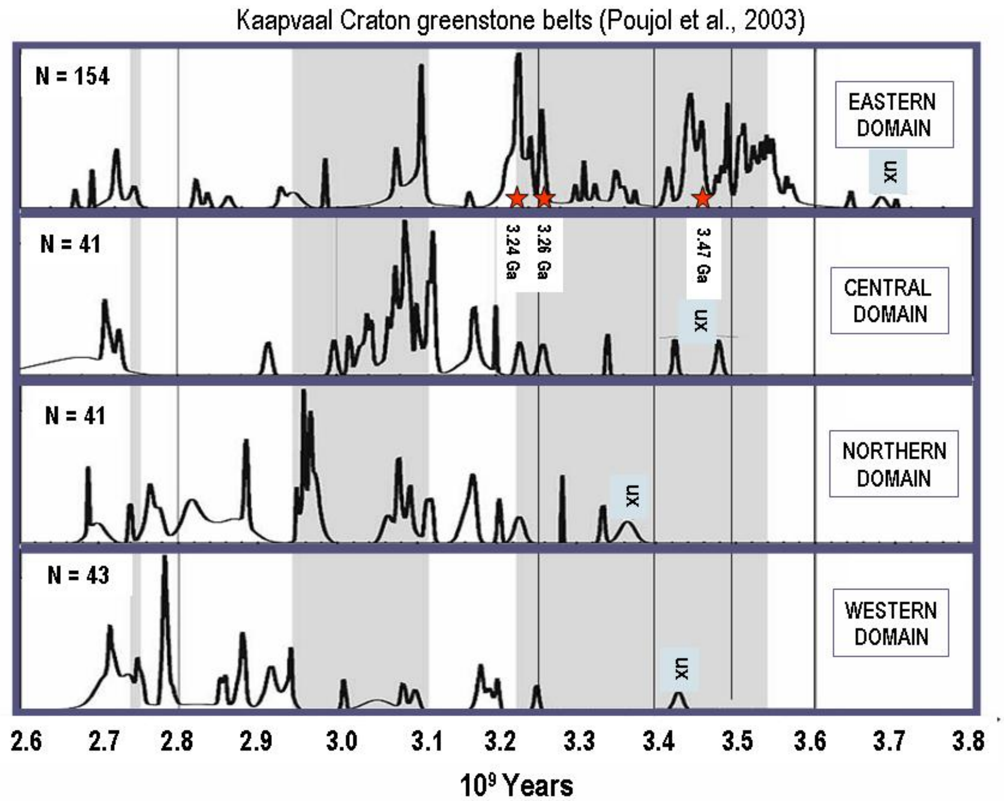

Figure 10

Age relative probabilities histogram for greenstone belts, Kaapvaal Craton, South Africa (after Poujol et al., 2003). Stars denote asteroid impact events.

Fig. 11

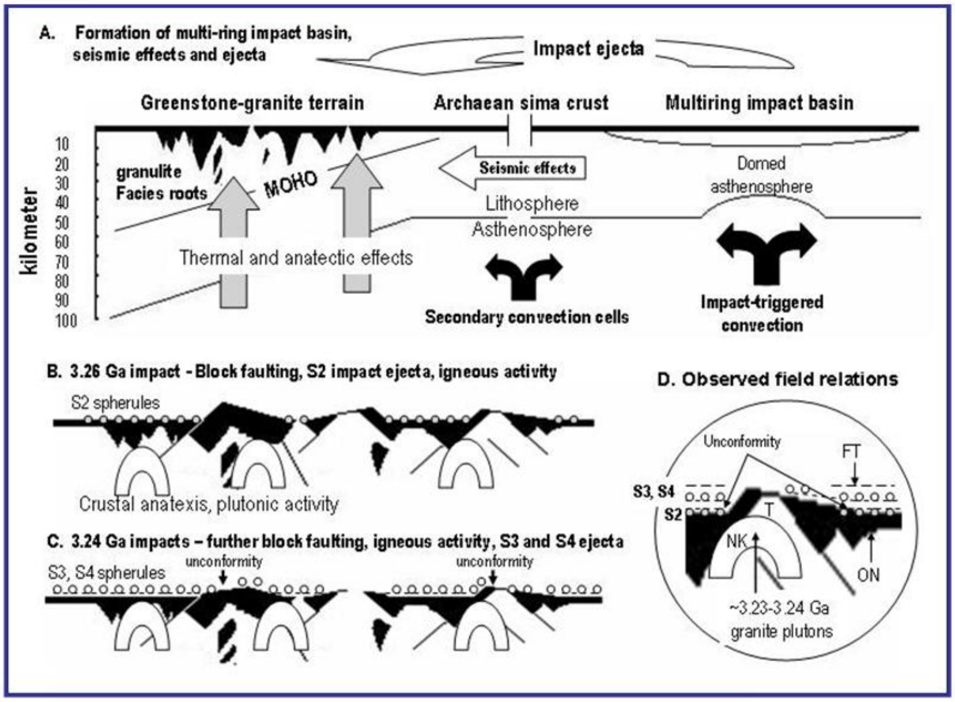

Figure 11

A model (not to scale) portraying the principal stages in multiple 3.26 and 3.24 Ga impacts in an oceanic region of the Achaean Earth and their geodynamic consequences, including formation of oceanic impact maria, mantle rebound and volcanic activity, ensuing rearrangement of mantle convection patterns, seismic activity affecting pre-existing granite-greenstone sial nuclei (microcontinent), faulting, uplift, erosion and formation of unconformities, anatexis at the roots of sial nuclei and rise of granitoid magmas.

A. ~3.26 Ga – Formation of a multi-ring impact basin by a ~20 km asteroid, seismically triggered faulting, mantle rebound and onset of a new convection cell, thermal and anatectic effects across the asthenosphere-lithosphere boundary below sial nuclei.

B. ~3.26 Ga: Block faulting in sial nuclei, rise of anatectic granites, settling of S2 ejecta spherules, preservation of S2 spherules preserved in below-wave base environments.

C. ~3.24 Ga – S3 and S4 impacts, ejecta fallout and preservation in below-wave base environments, further faulting, block movements and rise of plutonic magmas.

D. Schematic representation of observed field relations between the ~3.55-3.26 Ga mafic-ultramafic volcanic Onverwacht Group (ON), intrusive early tonalites and trondhjemites (T), 3.26-3.24 Ga granites (NK), S2 ejecta, unconformity, S3, S4 ejecta, and the Fig Tree Group sediments (FT).

TABLES

Table 1. Phanerozoic stage boundaries, large asteroid impacts and correlated volcanic and tectonic events. Note: no genetic connection is necessarily implied in this paper between age-correlated events.

Stage boundaries/epochs	Large asteroid impacts	large volcanic provinces
Mid-Miocene Langhian 15.97 Ma	Ries (24 km) 15.1±1.0 Ma	Columbia Plateau Basalt 16.2±1 Ma
Eocene–Oligocene boundary 33.9±0.1 Ma	Popigai (100 km) 35.7±0±2 Ma; Chesapeake Bay (85 km) 35.5±0.3 Ma	Ethiopin Basalts 36.9±0.9 Ma
KT boundary 65.5±0.3 Ma	Chicxulub (170 km) 64.98±0.05 Ma; Boltysh (25 km) 65.17±0.64 Ma	Deccan Plateau Basalts. 65.5±0.7 Ma (pooled Ar Ages: 65.5±2.5 Ma)
Cenomanian–Turonian 93.5±0.8 Ma	Steen River (25 km) 95±7 Ma	Madagascar Basalts 94.5±1.2 Ma
Aptian (Lower Cretaceous) 125 – 112 Ma	Carlswell (39 km) 115±10 Ma; Tookoonooka (55 km) 128±5 Ma; Tallundilli (30 km) 128±5 Ma; Mien (9 km) 121±2.3 Ma; Rotmistrovka (2.7 km) 120±10 Ma	Ontong-Java LIP 120 Ma; Kerguelen LIP 120–112.7–108.6 Ma; Ramjalal Basalts 117±1 Ma
End-Jurassic 145.5±4 Ma	Morokweng (70 km) 145±0.8 Gosses Bluff (24 km) 142.5F0.8 Ma; Mjolnir (40 km) 143F2.6 Ma	Dykes SW India 144±6 Ma
End-Pliensbachian 183±1.5 Ma		Peak Karoo volcanism Start 190±5 Ma; Peaks 193, 178 Ma; Lesotho 182±2 Ma
End-Triassic 199.6±0.3 Ma	Manicouagan (100 km) 214±1 Ma; Rochechouart (23 km) 213±8 Ma;	Central Atlantic Igneous Province: 203±0.7 to 199±2 Ma; Newark Basalts 201±1 Ma
Permian–Triassic 251±0.4 Ma 251.4±0.3 to 250.7±0.3 Ma	Araguinha (40 km) 252.7±3.8 Ma,	Siberian Norilsk 251.7±0.4 to 251.1±0.3 Ma
Late to end Devonian ~374–359 Ma	Woodleigh (120 km) 359±4 Ma; Siljan (52 km) 361±1.1 Ma; Alamo breccia (~100 km) ~360 Ma; Charlevoix (54 km) 342±15 Ma	Rifting and 364 Ma Pripyat–Dneiper–Donets volcanism
End-Ordovician 443.7±1.5 Ma	Several small poorly dated impact craters	
End-lower Cambrian 513±2 Ma		Kalkarindji volcanic Province, northern Australia 507F±4 Ma

Table 2. Early Precambrian asteroid impact fallout units and impact structures.

Geological unit	composition	Reference
3470.1±1.9 Ma: ACM-1, Antarctic Creek Member, Mount Ada Basalt, Warrawoona Group, Pilbara Craton	Silica-sericite spherules in ~1 meter-thick chert breccia/ conglomerate. Overlain by felsic hypabyssal/volcanics	Byerly et al., 2002
3470.1±1.9Ma: ACM-2, Antarctic Creek Member, Mount Ada Basalt, Warrawoona Group, Pilbara Craton	Silica-sericite spherules within ~14 meter-thick chert, arenite. Overlain by ~ 10 meters-thick jaspilite overlying spherule unit ACM-1	Byerly et al., 2002
3470.4±2.3 Ma: BGB-S1A & BGB-S1B, upper Hooggenoeg Formation, Onverwacht Group, Kaapvaal Craton	Two units of silica-chert spherules within 30-300 cm thick unit of chert and arenite.	Byerly et al., 2002
3258±3 Ma: BGB-S2, base of the Mapepe Formation, Fig Tree Group, Kaapvaal Craton	<310 cm-thick Silica-sericite spherules. Overlain by Manzimnyama Jaspilite Member:: BIF+ jaspilite +Ferruginous shale (<20 m) and shale common above BGB-S2	Lowe et al., 2003
3243±4 Ma to 3225±3 Ma: BGB-S3 and BGB-4, lower Mapepe Formation, Fig Tree Group, Kaapvaal Craton	S3 - 10-15 cm-thick to locally 2-3 meters-thick silica-Cr sericite-chlorite spherules, overlain by ferruginous sediments of the Ulundi Formation in the northern part of the BGB. S4 - 15 cm-thick arenite with chlorite-rich spherules	Lowe et al., 2003
2629±5Ma (?): JIL, top Jeerinah Formation, Fortescue Group, Hamersley Basin.	Hesta - 80 cm-thick carbonate-chlorite spherules and spherule-bearing breccia; 60 cm thick overlying debris flow. Overlain by Marra Mamba Iron-formation, immediately above ~60 cm-thick shale unit overlying JIL	Simonson et al. 2000; Trendall et al. 2004
2630±6 Ma, base of Carawine Dolomite, Hamersley Group, Hamersley Basin	Carbonate megabreccia-hosted microkrystite spherules. K-feldspar-carbonate-chlorite spherules in tsunami-generated carbonate-chert megabreccia.	Rasmussen et al. 2005
?2.63 Ga: Monteville Formation, West Griqualand Basin, west Kaapvaal Craton	5 cm-thick spherule layer. Carbonate hosted	Simonson and Glass, 2004
?2.56 Ga: Reivilo Formation, West Griqualand Basin, western Kaapvaal Craton.	1.8 cm-thick spherule unit. Carbonate-hosted	Simonson and Glass, 2004
2562±6 Ma: SMB-1, top of Bee Gorge Member, upper Wittenoom Formation, Hamersley Group, Hamersley Basin	<5 cm-thick K feldspar-carbonate-chlorite spherules in carbonate turbidite. Overlain by Ferruginous siltstone (Sylvia Formation), banded iron formations (Bruno Member)	Simonson, 1992; Trendall et al, 2004
2562±6 Ma: SMB-2, top of Bee Gorge Member, upper Wittenoom Formation, Hamersley Group, Hamersley Basin	<20 cm-thick K feldspar carbonate-chlorite spherules within turbidite. Overlain by ferruginous siltstone (Sylvia Formation), banded iron formations (Bruno Member)	Glikson, 2004; Trendall et al., 2004
2481±4 Ma: S4, Shale Macroband, Dales Gorge Member, Brockman Iron-formation, Hamersley Group, Hamersley Basin	10-20 cm K feldspar-stilpnomelane spherules at top of 2-3 meters of ferruginous volcanic tuffs. Located 38 meters above the base of the Brockman Iron-formation, Hamersley Basin.	Trendall et al., 2004
~2.5-2.4 Ga: lower Kuruman Formation, West Griqualand Basin, west Kaapvaal Craton	1 cm-thick spherule unit overlain by 80 cm breccia. Located 37 meters above base of banded ironstones	Simonson and Glass, 2004
2.023±4 Ga: Vredefort impact		Kamo et al., 1996.

structure, Transvaal.		
1.85-2.13 Ga: Graensco, Vallen, Ketilidean, southwest Greenland	20 cm-thick spherule unit. Carbonate-hosted spherules	Chadwick et al., 2001
1850±1 Ma Sudbury impact structure D~250 km		Davis, 2008; Addison et al., 2005

Table 3. Geological elements associated with, or overlapping, asteroid impact ejecta units

Impact event (Ga)	**Unconformities or para-conformities**	**Breccia**	**tsunami**	**Change in Sedimentary facies**	**Igneous Events** (age overlap)
~3.47 Ga [1, 2]	?	V	V	Overlying jaspilite [2]	
~3.26 [3, 4]	V	V	V	Overlying turbidite and BIF	
~3.24 [4]	V	V	V	Overlying turbidite and BIF	3.227±1 KVP 3.236±1 NT
~2.63 (?) [5]	?	V	V	Overlying BIF	
~2.56 [6, 7]	?		V	Overlying Fe-Shale, BIF	
~2.48 [8]			V	Within BIF	

Referneces: [1] Byerly et al., 2002; [2] Glikson et al., 2004; [3] Lowe et al., 2003; [4] Glikson and Vickers, 2005 (KPV – Kaap Valley Pluton; NT – Nelshoogte Tonalite); [5] Simonson et al., 2000; [6] Simonson, 1992; [7] Glikson and Vickers, 2006; [8] Glikson and Allen, 2004.